A New Molecular Model for Collagen Elasticity Based on Synchrotron X-Ray Scattering Evidence

Klaus Misof,* Gert Rapp,# and Peter Fratzl*
*Institut für Materialphysik der Universität Wien and Ludwig Boltzmann-Institut für Osteologie, A-1090 Vienna, Austria, and #European Molecular Biology Laboratory, 22603 Hamburg, Germany

ABSTRACT Collagen is the most abundant structural protein in vertebrates. The specific shape of its stress-strain curve is crucial for the function of a number of organs. Although the macroscopic mechanical behavior of collagen is well known, there is still no explanation of the elastic process at the supramolecular level. We have performed in situ synchrotron x-ray scattering experiments, which show that the amount of lateral molecular order increases upon stretching of collagen fibers. In strain cycling experiments the relation between strain and diffuse equatorial scattering was found to be linear in the "heel" region of the stress-strain curve. A new molecular model for collagen elasticity is proposed, which, based on the existence of thermally activated molecular kinks, reproduces this linearity and gives a simple explanation for the form of the stress-strain curve of collagen.

INTRODUCTION

Collagen type I is the most abundant structural protein in vertebrates, and its mechanical properties are essential for the function of a number of organs, like tendons or arteries. Many of these properties are due to the shape of the stress-strain curve of collagen, which is characterized by a region of relatively low elastic modulus at small strains ("toe region") followed by an upward bend of the curve ("heel region") and, finally, a linear region with high elastic modulus at large strains (Vincent, 1990; Silver et al., 1992). Despite its importance to the mechanical function of collagen, there is still a lack of understanding of the correlation between the specific shape of the stress-strain curve and the deformations of collagen at the molecular level.

The toe region of the stress-strain curve had been linked to a macroscopic crimp with a period of about 100 μm (Silver et al., 1992; Abrahams, 1967) or shorter (Dale and Baer, 1974), found systematically in unstretched collagen fibers by polarized light microscopy. In tendons this crimp disappears upon stretching at extensions of (typically) 4% (Silver et al., 1992; Abrahams, 1967), a value that may depend on the age of the animal (Diamant et al., 1972). At larger strains, x-ray diffraction measurements (Mosler et al., 1985; Folkhard et al., 1986) of the axial molecular packing (Hodge and Petruska, 1963) were interpreted as a side-by-side gliding of the molecules, accompanied by a stretching of the cross-linked telopeptide terminals and a stretching of the triple helices themselves (Mosler et al., 1985). A further complication may also arise from the fact that the molecules are not arranged parallel to the fibril direction, but rather with a tilt of about 5° (Fraser et al., 1983), so that stretching could also be related to a straightening out of the molecule direction. Because such mechanisms must involve large tensile forces, they are likely to play an important role at large strains, in the linear regime of the stress-strain curve. Moreover, none of them gives a satisfactory explanation for the heel region at intermediate strains.

Even though the axial packing of collagen fibrils is known to be highly regular (Hodge and Petruska, 1963), there is a large amount of disorder in the structure, mostly in the lateral packing of the molecules (Brodsky et al., 1982). At least for rat tail tendon (RTT), x-ray scattering reveals crystalline regions in the fibrils (Miller and Wray, 1971; Katz and Li, 1973), but also indicates the existence of regions with an almost liquid arrangement of the molecules (Woodhead-Galloway and Young, 1978; Hulmes et al., 1995). They probably correspond to the gap regions of the fibrils, where the molecular density is reduced by 20% with respect to the overlap regions (Fraser et al., 1983). There is also a considerable flexibility of the molecules in the gap regions both azimuthally and laterally, as demonstrated by NMR (Jelinski et al., 1980) as well as x-ray diffraction (Fraser and Trus, 1986). Consequently, it would be natural to expect that tensile stress could affect the lateral mobility of the molecules and, hence, the amount of order in the liquid-like structure. Conversely, a change in disorder (and, therefore, entropy) would exert a force contributing to elasticity, a well-known property, e.g., in the case of rubbers (Ullman, 1993; Flory, 1953). To investigate this possibility, we have undertaken a synchrotron x-ray scattering study of the changes in lateral order upon axial stretching of collagen.

MATERIALS AND METHODS

Sample preparation

Fibers (diameter 100–200 μm) were dissected from 8-week-old rattail tendons and immediately stored in physiological phosphate-buffered saline (PBS) solution at 4°C. Some tendons were tested just after dissection, others after storage in PBS for 2–3 days. No differences in the equatorial scattering or in the stress/strain data could be observed between samples

Received for publication 17 June 1996 and in final form 2 December 1996.
Address reprint requests to Dr. Peter Fratzl, Institut für Materialphysik, Strudlhofgasse 4, A-1090 Vienna, Austria. Tel.: 43-1-313-67-3242; Fax: 43-1-310-0183; E-mail: fratzl@pap.univie.ac.at.

0006-3495/97/03/1376/06 $2.00

that were examined immediately after dissection and the others, which were stored in PBS for some days. To investigate collagen fibers under controlled strain and stress conditions, a special apparatus was built for in situ synchrotron x-ray scattering experiments. Fig. 1 shows a schematic diagram of the apparatus. The fibers were clamped vertically between two grips, which could be moved by a DC micrometer drive. For measuring the tensile force, a small load cell was directly mounted on one grip, and the strain was recorded by means of a transducer that was connected to the grips. Both the signal of the load cell and that of the transducer were recorded by a computer. The minimum detectable load was about 0.2 g. To keep the rattail tendon collagen in native condition, the whole stretching device was enclosed in a container with PBS solution.

X-ray measurements

The x-ray scattering experiments were performed using a beamline of the EMBL Outstation, Hamburg, at DESY (Deutsches Electron Synchrotron). In each case, the apparatus was mounted on an optical bench in such a way that the axial direction of the collagen fibers was perpendicular to the incoming x-ray beam. The windows for the x-ray beam consisted of 70-μm Mylar foils. During the x-ray experiments the solution level was lowered just below the x-ray beam, in such a way that part of the specimen stayed immersed in the physiological solution. The fibers were stretched to the point where the first force was detected. The length of the fibers at this point was assumed to be the initial unstretched length (typically about 12.3 mm). A fast-readout linear position-sensitive detector (Rapp et al., 1995) positioned at a distance 28 cm from the specimen was used to record the diffuse equatorial scattering $I(s)$ from $s = 0.22\ \text{nm}^{-1}$ to $1.18\ \text{nm}^{-1}$, where $s = 2/\lambda \sin\theta$ ($\lambda = 1.5$ Å), where 2θ is the scattering angle. The height of the entrance window of the detector was 8 mm, making it possible to integrate over the entire equatorial scattering at the distance of 28 cm. The strain rate for each experiment was about 0.007%/s. Before the cycles, a 2D diffraction pattern of the unstretched specimen was collected on an image plate and analyzed with the in-house software SCACO.

RESULTS

In a series of experiments the strain of unstretched collagen fibers was first raised to a given value (typically 5%) and then lowered again. A second cycle then did not start at strain = 0, but at the point where further extension of collagen led to a measurable stress. In this way, the succession of several such cycles led to a typical total strain of 8–10%. From this point on, the stress-strain relation had only a very small hysteresis, and the collagen behaved elastically, with a stress-strain curve still bent upward. Further cycles were performed in this stage within the heel region of the stress-strain curve. Fig. 2 shows the corresponding variation of the equatorial diffuse x-ray scattering intensity $I(s)$ as a function of time, together with the variation of the strain. The duration of one cycle was typically 16 min, during which 20 x-ray patterns were taken. Fig. 2 shows seven cycles, and a reversible intensity increase with increasing strain is clearly observable. The maximum of the diffuse peak was observed at $s = 0.72\ \text{nm}^{-1}$, which corresponds to a typical distance of the collagen molecules of about 1.38 nm. No shift in the peak maximum of the equatorial scattering was observed, which would be expected if testing would induce dehydration of the specimen (Fratzl et al., 1993). This means that the molecular order increased under tension, but that the average molecular spacing remained unchanged.

Three quantities were determined during the experiment and are shown as a function of time on the left of Fig. 3. Fig. 3 *A* gives the strain, Fig. 3 *B* the tension, and Fig. 3 *D* the maximum equatorial scattering intensity. As visible in Fig. 3 *A*, the strain was increased and decreased linearly in time (with a strain rate of $7 \times 10^{-5}\ \text{s}^{-1}$) in several cycles. The first data point of each cycle corresponds to the moment at which the first measurable stress occurred in the specimen when the tendon was stretched. The cycles can also be seen in Fig. 3 *B*, where the tension is plotted. The tension also increased and decreased in each cycle, however, in a fashion totally different from the strain. First, there was no systematic (irreversible) increase from cycle to cycle as in Fig. 3 *A*, and then the tension "pulses" were much shorter than the strain "pulses." It is also worth noting that starting from cycle 4, both stress and strain data were reversible (there was no more systematic increase of the strain from one cycle to the next). Moreover, the maximum stress was about

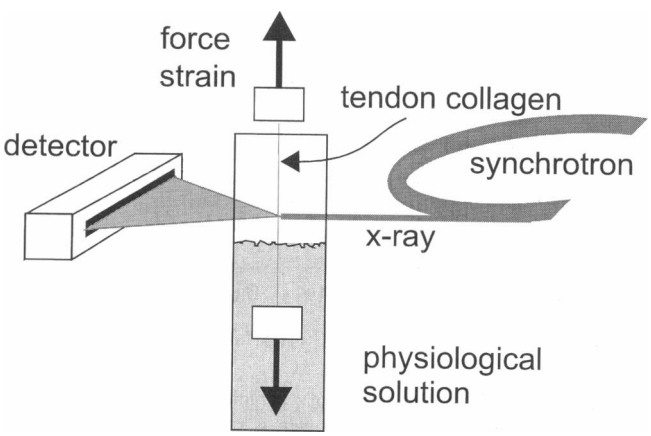

FIGURE 1 Schematic diagram of the experimental apparatus for the x-ray measurements.

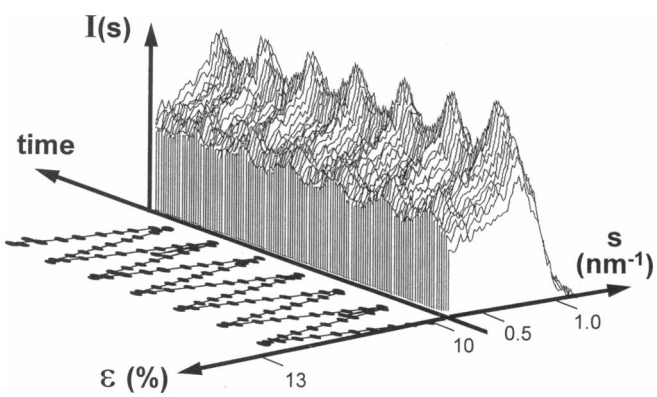

FIGURE 2 Variation of the equatorial diffuse x-ray scattering intensity $I(s)$ as a function of time, together with the variation of strain ϵ. The duration of one cycle was 16 min. Seven strain cycles with the same sample are plotted between 10% and 13%. At the same time the equatorial scattering was detected and is also shown on this diagram between s = 0.22 nm^{-1} and 1.18 nm^{-1}, where $s = 2/\lambda \sin\theta$, ($\lambda = 1.5$ Å). The exposed time for one spectrum was 50 s.

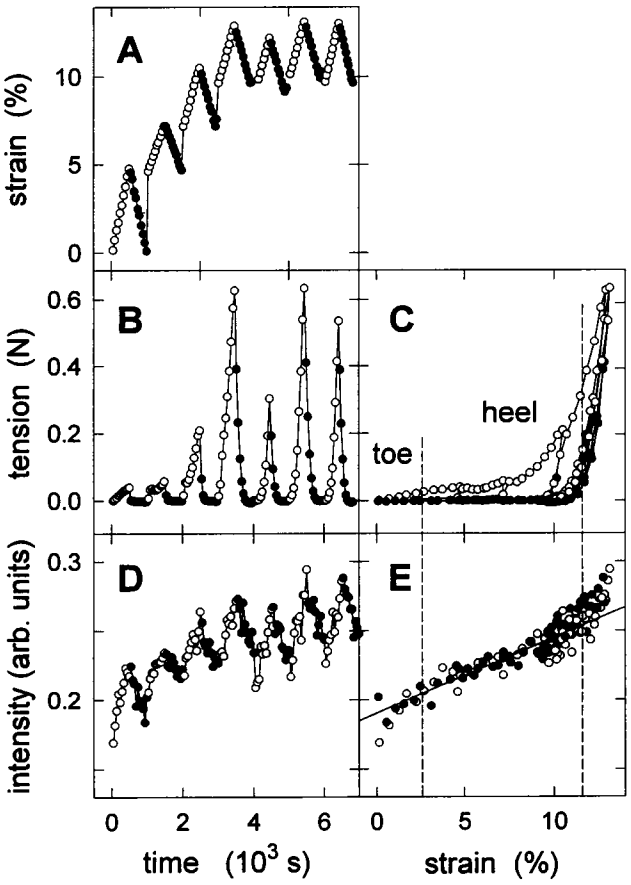

FIGURE 3 On the left side strain, stress and intensity $I(s)$ at s = 0.72 nm^{-1} are plotted versus time in *A*, *B*, and *D*, respectively, and on the right side versus strain in *C* and *E*, obtained from seven successive stress-strain cycles up to ϵ = 13%. Data points obtained with increasing strain are shown by open symbols, with decreasing strain by closed symbols. (*A*) The strain was increased and decreased linearly in time in each cycle. The first data point of each cycle corresponds to the moment where the first measurable stress occurred in the specimen when the fiber was stretched. (*B*) It is evident that the tension falls to zero much faster than the strain in the second half of each cycle. (*C*) It is visible that the data points from cycles 4 to 7 superimpose on that graph. The data points obtained with decreasing strain (●) are always on the lower curve, showing that the stress relaxes much faster than the strain when tension on the fiber is released. (*D*) The maximum x-ray scattering intensity shows a general behavior that closely resembles that of the strain. (*E*) All data points lie on one continuous curve. The dotted lines mark the region over which the relation between strain and x-ray intensity is linear.

the same for cycles 4, 6, and 7, in which the maximum strain was the same. A lower maximum strain (as in cycle 5) led to a smaller maximum stress.

To get a better visualization of the relation between these two quantities, we have plotted tension versus strain in Fig. 3 *C*. It is apparent that the data from cycles 4 to 7 superimpose on that graph, showing the reversibility of the stress-strain curve under these conditions. Moreover, all data points obtained with increasing strain (*open symbols*) form a continuous curve, even though they were obtained in successive cycles, e.g., the first cycle up to a strain of 5%, the second between 5% and 7.5%, etc. (Fig. 3 *A*). However, the data points obtained with decreasing strain (*closed symbols*) are always on the lower curve, showing that the stress relaxed much faster than the strain when the tension on the specimen was released.

A third quantity, the maximum x-ray scattering intensity, is shown in Fig. 3 *D* as a function of time. Again, the seven cycles are clearly visible. However, in contrast to the stress (Fig. 3 *B*), the intensity (Fig. 3 *D*) showed an irreversible increase between the cycles and a general behavior that closely resembles that of the strain. To highlight this point, we have finally plotted the intensity versus strain in Fig. 3 *E*. The most surprising result is that all of the different strain cycles lie on the same curve, which is linear in the region of 4–12% strain. There are no differences even between data points obtained with increasing (*open symbols*) or decreasing (*closed symbols*) strain.

To get an idea of the nature of the molecular ordering corresponding to the increase in total x-ray scattering intensity (Fig. 3 *D*), we have also analyzed the change in the shape of the diffuse scattering maximum. An example of this is shown in Fig. 4 for two very different strain values. First, there is no visible shift of the diffuse maximum. This shows that the average position of the molecules in the lateral packing of the fibrils stayed roughly the same. Hence the disorder must correspond to a random deviation of the molecules from their average positions. If the increase in order was due to a closer packing of the molecules, there would be a shift of the maximum, as would occur, e.g., upon drying (Fratzl et al., 1993). A ratio of the intensities in Fig.

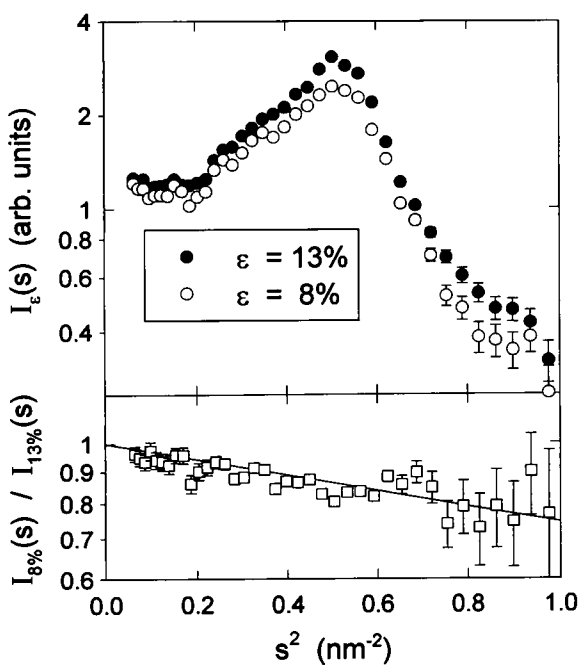

FIGURE 4 The equatorial scattering $I(s)$ plotted on a logarithmic scale for two typical strains, 8% and 13%, versus s^2. In the lower part of the diagram, the difference between the two curves (corresponding to the logarithm of the ratio Q of the intensity at 8% and 13%) is plotted versus s^2. The straight line corresponds to a fit of the ratio Q with $\exp(-\mu s^2)$.

4 shows further that the intensity change can be fully accounted for by a Debye-Waller factor (Azároff, 1968):

$$I(s) = I_0(s) \exp(-\mu s^2), \quad (1)$$

where μ is the only parameter that varies in a given strain cycling experiment.

DISCUSSION

Three observations clearly emerged from the experiment:

1. When tension is released, the stress disappears immediately, but the strain takes a much longer time to relax (hysteresis in Fig. 3 *C*). This indicates that a very slow (and, therefore, probably thermally activated) process contributes to the shortening of the tendon.

2. The equatorial x-ray scattering intensity, which is a measure of the lateral ordering of the molecules in the collagen fibrils, is a direct function of the tensile strain on the tendon (Fig. 3 *D*). The actual state of stress has no influence on the lateral order, as long as the strain is the same. Hence there must be a direct connection between the length of the tendon and the lateral order of the molecules. It is therefore very likely that the process mentioned in 1 is related to lateral ordering of the molecules.

3. All changes in the x-ray scattering curves can be accounted for by changes in the Debye-Waller factor, which measures the amount of random deviations of the molecules from their fixed average positions.

These three facts clearly point to a mechanism for collagen elasticity in which random deviations of the molecules from their average positions lead to a shortening of the fibrils. When tension is applied to the tendon, a part of the elongation should then be due to the removal of this disorder, which implies an entropic origin for the elastic forces. In the following, we propose a very simple model that is able to account for all of our observations.

A new molecular model

A simple assumption leading to a random deviation of the molecules from their average position would be the existence of microkinks in the molecules, which have already been proposed to explain the absence of certain reflections in the diffraction pattern from collagen (Fraser et al., 1987). Indeed, if there is no external stress on the molecules, certain molecular segments of length ℓ (probably located in the hole zone) with a particular sequence of amino acids (Fraser and Trus, 1986) may be sufficiently mobile to form microkinks, as shown schematically in Fig. 5. This would lead to a reduction $\delta\ell$ in the length of the molecule, where δ is related to the lateral excursion $\underline{u}$ within the equatorial plane by the formula given in Fig. 5. When a tensile force f acts on the molecule (see Fig. 5), the work required to remove the kink is $E = f\delta\ell = 2f\underline{u}^2/\ell$. The formation of kinks with the vector u pointing into a random direction within the equatorial plane will increase the lateral disorder

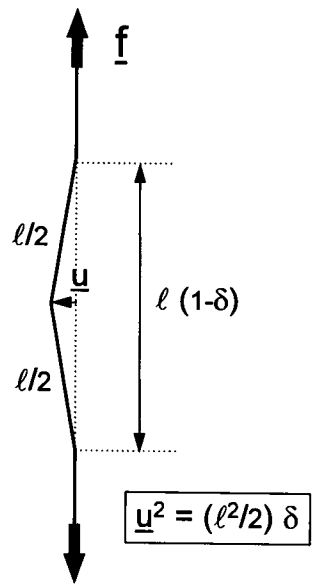

FIGURE 5 Schematic model for a microkink of length ℓ in the collagen molecule. u is the lateral excursion of the molecule within the equatorial plane, and $\delta\ell$ is the corresponding reduction in length of the molecule.

and, hence, the entropy of the fibril. Therefore, assuming that, for a given type of kink, ℓ is fixed but u is random ($\underline{u}$ being a planar vector), the energy E (proportional to $\underline{u}^2$) has the same form as a harmonic oscillator with two degrees of freedom. Therefore, the average energy $\langle E\rangle$ at the temperature T will be $\langle E\rangle = kT$ (where k is the Boltzmann constant). Consequently,

$$\langle E\rangle = kT = f\ell\langle\delta\rangle = (2f/\ell)\langle\underline{u}^2\rangle. \quad (2)$$

These very simple equations may now be used to derive a stress-strain relationship for the collagen fibril. Assuming that with no external stress the average value $\langle\delta\rangle$ is equal to δ_0, a strain ϵ would correspond to

$$\varepsilon = \nu\ell/D\,(\delta_0 - \langle\delta\rangle), \quad (3)$$

where we have called D the length of the axial collagen period after removal of all kinks and ν the total number of kinks of a molecule per D-period. With the tensile force being given by Eq. 2, it follows for the external stress σ that must be applied to achieve a strain ϵ that

$$\sigma = \rho\,(kT/\ell\langle\delta\rangle - kT/\ell\delta_0) \quad (4)$$

where ρ is the number of molecules per unit surface in the equatorial plane. Finally, inserting Eq. 3 into Eq. 4, one gets

$$\sigma = K\epsilon/(1 - \epsilon/\epsilon_0), \quad (5)$$

with

$$\epsilon_0 = \nu\ell\delta_0/D$$

and

$$K = \rho kT\nu/(\epsilon_0^2 D).$$

Hence when ϵ is small compared to ϵ_0, the prediction is a linear elastic behavior with the elastic modulus K. When ϵ approaches ϵ_0 (that is, when almost all of the kinks are removed), the tension σ required to get a further extension by removal of the remaining kinks diverges, which means that other mechanisms must become dominant for the elastic behavior. The stress-strain curve corresponding to Eq. 5 is bent upward and is, in fact, an excellent description of the one for collagen in the heel region (*between the two dotted vertical lines* in Fig. 3 *C*). When σ predicted by Eq. 5 becomes too large, it is very likely that other mechanisms of collagen elasticity, like a direct stretching or a side-by-side gliding (Mosler et al., 1985; Folkhard et al., 1986) of the molecules, come into play and lead to a linear stress-strain relation instead of the divergence predicted by Eq. 5.

It is important to note that the linear relation between the strain of the collagen fiber and the amount of lateral molecular disorder, as measured by the diffuse x-ray scattering intensity (Fig. 2 *E*), also follows directly from Eq. 2. Describing the effect of lateral disorder on the x-ray scattering intensity $I(s)$ by a Debye-Waller factor (Azároff, 1968), as motivated by Fig. 4 and Eq. 1, one gets

$$I(s) = I_0(s)\exp(-4\pi^2 s^2\langle \underline{u}^2\rangle) \approx A - B\langle \underline{u}^2\rangle \approx A' + B'\epsilon, \tag{6}$$

where the constants are $A = I_0(s)$, $B = 4A\pi^2 s^2$, $B' = B\ell D/(2\nu)$, and $A' = A - B'\epsilon_0$. In agreement with the experimental observation, a linear relation is predicted by Eq. 6 between the intensity at a given s and the measured strain ϵ. This corresponds to the portion of Fig. 3 *E* between the two dotted vertical lines.

Quantitative comparison to the experiment

Although there is an excellent qualitative agreement between model and experiment, a quantitative comparison is difficult because the model is probably oversimplified and because not all parameters are known with the required accuracy. To estimate at least the orders of magnitude, we have converted the tension-strain diagram for a typical fibril by taking a circular cross section of 200 μm (Fig. 6). This value was determined by measurements made with a light microscope at various positions along the fibril and is affected by rather large errors. Consequently, the absolute scale on the ordinate in Fig. 6 can only be regarded as an order of magnitude.

A further difficulty for a quantitative comparison lies in the fact that a macroscopic crimp (Fig. 1) is removed before the mechanism described in this paper becomes operational. To account for this fact, we have fitted the stress-strain curve in the heel region (*full symbols* in Fig. 6) by using Eq. 5, where the strain ϵ was replaced by $\epsilon - \epsilon_M$, where ϵ_M is the strain due to removal of the macroscopic crimp. The result of the fit was

$$\epsilon_M \approx 2\%, \quad \epsilon_0 \approx 11\% \quad \text{and} \quad K \approx 19\ \text{MPa}.$$

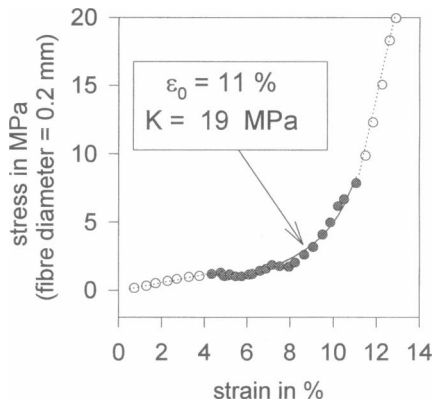

FIGURE 6 The stress is plotted versus strain for a typical rattail tendon of diameter ~200 μm. The stress is calculated assuming a circular cross section of the fibers with a 0.2-mm diameter. The solid line is a fit with Eq. 5 through the closed symbols. The dashed line at low strain marks the region where the macroscopic crimp is removed. At strain over about ϵ_0, Eq. 5 diverges and other mechanisms for collagen elasticity become dominant.

Hence the elastic modulus K is considerably larger than values for natural rubber, which are on the order of 1 MPa (Ullman, 1993; Flory, 1953). To get an estimate for K from our model, one can use the fact that $K\epsilon_0^2 = \rho kT\nu/D$ from Eq. 5. Using $T = 27°C$, $\rho = 4.89 \times 10^{17}\ m^{-2}$ (Hulmes et al., 1995), and $D \approx 68$ nm, one obtains $\rho kT/D \approx 3 \times 10^4$ Pa. Because from the experiment $K\epsilon_0^2 \approx 2 \times 10^5$ Pa, there would be quantitative agreement if $\nu \approx 7$, which means that there should be about seven kinks per D-period for each molecule in the fibril. Even though this value should not be taken too seriously because of the large uncertainties in all of the estimates, the order of magnitude is quite reasonable.

CONCLUSION

The equatorial x-ray scattering from rattail tendon collagen has been analyzed as a function of strain and stress. The experiments reveal a linear relation between the strain and the integral intensity of the equatorial scattering, which can be explained by a lateral ordering process in the fibrils. The experimental results led to the development of a new molecular model based on the existence of thermally activated kinks in the collagen molecules, which are stretched out when tension is applied to the tendon collagen. Consequently, the existence of thermally activated kinks in the collagen molecules can explain not only the strict linearity between the strain and the diffuse equatorial intensity (Fig. 3 *E*), but also the shape of the stress-strain curve in the heel region (Fig. 3 *C*) found in the present experiment. Hence we are confident that microkinks are, indeed, the origin of the entropic elasticity of collagen fibers. Finally, it may be noted that the theoretical stress-strain relation (Eq. 5) also predicts a clear temperature dependence of the elasticity (via the constant K), which may be exploited in future experiments.

REFERENCES

Abrahams, M. 1967. Mechanical behaviour of tendon in vitro. *Med. Biol. Eng.* 5:433–443.

Azároff, L. V. 1968. Elements of X-ray Crystallography. McGraw-Hill, New York. 234–243.

Brodsky, B., E. F. Eikenberry, K. C. Belbruno, and K. Sterling. 1982. Variations in collagenfibril structure in tendons. *Biopolymers.* 21: 935–951.

Dale, W. C., and E. Baer. 1974. Fibre-buckling in composite systems: a model for the ultrastructure of uncalcified collagen tissues. *J. Mater. Sci.* 9:369–382.

Diamant, J., A. Keller, E. Baer, M. Litt, and R. G. C. Arridge. 1972. Collagen: ultrastructure and its relation to mechanical properties as a function of aging. *Proc. R. Soc. Lond. B.* 180:293–315.

Flory, P. J. 1953. Principles of Polymer Chemistry. Cornell University Press, Ithaca, NY.

Folkhard, W., E. Mosler, W. Geercken, E. Knörzer, H. Nemetschek-Gonsler, Th. Nemetschek, and M. H. J. Koch. 1986. Quantitative analysis of the molecular sliding mechanism in native tendon collagen-time-resolved dynamic studies using synchrotron radiation. *Int. J. Biol. Macromol.* 9:169–175.

Fraser, R. D. B., T. P. MacRae, and A. Miller. 1987. Molecular packing in type I collagen fibrils. *J. Mol. Biol.* 193:115–125.

Fraser, R. D. B., T. P. MacRae, A. Miller, and E. Suzuki. 1983. Molecular conformation and packing in collagen fibrils. *J. Mol. Biol.* 167:497–521.

Fraser, R. D. B., and B. L. Trus. 1986. Molecular mobility in the gap regions of type I collagen fibrils. *Biosci. Rep.* 6:221–226.

Fratzl, P., N. Fratzl-Zelman, and K. Klaushofer. 1993. Collagen packing and mineralization. *Biophys. J.* 64:260–266.

Hodge, A. J., and J. A. Petruska. 1963. Recent studies with the electron microscope on ordered aggregates of the tropocollagen molecule. *In* Aspects of Protein Structure. G. N. Ramachandran, editor. Academic Press, New York. 289–300.

Hulmes, D. J. S., T. J. Wess, D. J. Prockop, and P. Fratzl. 1995. Radial packing, order and disorder in collagen fibrils. *Biophys. J.* 68: 1661–1670.

Jelinski, L. W., C. E. Sullivan, and D. A. Torchia. 1980. ^{2}H NMR study of molecular motion in collagen fibrils. *Nature.* 284:531–534.

Katz, E. P., and S. Li. 1973. Structure and function of bone collagen fibrils. *J. Mol. Biol.* 80:1–15.

Miller, A., and J. S. Wray. 1971. Molecular packing in collagen. *Nature.* 230:437–439.

Mosler, E., W. Folkhard, E. Knörzer, H. Nemetschek-Gonsler, Th. Nemetschek, and M. H. J. Koch. 1985. Stress-induced molecular rearrangement in tendon collagen. *J. Mol. Biol.* 182:589–596.

Rapp, G., A. Gabriel, M. Dosiere, and M. J. Koch. 1995. A dual detector single readout system for simultaneous small- (SAXS) and wide-angle x-ray (WAXS) scattering. *Nucl. Instrum. Methods A.* 357:178–182.

Silver, F. H., Y. P. Kato, M. Ohno, and A. J. Wasserman. 1992. Analysis of mammalian connective tissue: relationship between hierarchical structures and mechanical properties. *J. Long-Term Effects Med. Implants.* 2:165–195.

Ullman, R. 1993. Rubber elasticity. *In* Materials Science and Technology: Structure and Properties of Polymers, Vol. 12. R. W. Cahn, P. Haasen, and E. J. Kramer, editors. VHC Publishers, New York. 357–387.

Vincent, J. 1990. Structural Biomaterials. Princeton University Press, Princeton, NJ.

Woodhead-Galloway, J., and W. H. Young. 1978. Probabilistic aspects of the structure of the collagen fibril. *Acta Crystallogr. A.* 34:12–18.